Modeling Earth Systems and Environment
https://doi.org/10.1007/s40808-018-0479-0

ORIGINAL ARTICLE

Variable resolution modeling of near future mean temperature changes in the dry sub-humid region of Ghana

Enoch Bessah[1] · Abdulganiy O. Raji[2] · Olalekan J. Taiwo[3] · Sampson K. Agodzo[4] · Olusola O. Ololade[5]

Received: 7 February 2018 / Accepted: 23 May 2018

Abstract

The study used two models from Rossby Centre Regional Atmospheric Model (RCA4) and two from Weather Research and Forecasting Model (WRF) plus the Statistical Downscaling Model—Decision Centric (SDSM-DC) at 44 km, 12 km and 2 m resolution respectively to project the impact of climate change on mean temperature in the Pra River Basin for the period 2020–2049. Results showed that the minimum temperature increased (+ 1.47 °C) faster than the increase (+ 1.11 °C) in maximum temperature for observed period 1981–2010. An evaluation of the performance of the models with time-series based metrics showed that SDSM-DC and RCA4 are better for projecting mean temperature in the study area compared to WRF despite its resolution. Analysis of variance ($p < 0.05$) indicated significant difference between the projected mean temperature of the five models but there was no significant difference between SDSM-DC and RCA4 models. Correlation between models was highest at $R = 0.727$ between SDSM-DC and RCA4. The years 2041, 2042 and 2047 were projected as hottest by minimum two different models. The mean temperature change was projected at + 1.36, + 1.42 and + 1.12 °C by SDSM-DC, RCA4 and WRF respectively. The ensemble of projection depicted same trend of February—April as the high mean temperature and July—September as the lowest as was for the observed period. However, January is projected to have the highest change in mean temperature of + 1.51 °C. The maximum temperature for observed period was found to be the mean temperature in the period 2020–2049. Future study will focus on the impact of projected temperature change on ecosystem services delivery in the region.

Keywords Ghana · SDSM-DC · RCMs · RCP 4.5 scenario · Temperature · Model

Introduction

The Intergovernmental Panel on Climate Change (IPCC) fifth Assessment reports (AR5) shows a warming linear trend between 0.65 and 1.06 °C globally, over the period of 1880 to 2012 (IPCC 2014). They projected mean global temperature rise between 1.4 and 5.8 °C by the end of the twenty-first century in the third Assessment report (IPCC 2001). The increase in temperature was attributed to the doubling of the CO_2 concentration in the atmosphere. The temperature rise would impact on different socio-economic sectors in terms of productivity and resource availability. The first IPCC report on climate change (IPCC 1990) triggered great interest in climate modeling in order to understand climate mechanisms and assess climate evolution at short and long terms under different climate change scenarios (IPCC 2007; Vanvyve et al. 2008). The simulations are being implemented at different spatial scales, from the global, regional to the local scale through evolving models in

✉ Enoch Bessah
ebessah0180@stu.ui.edu.ng

1 Pan African University, Institute of Life and Earth Sciences (Including Health and Agriculture), University of Ibadan, Ibadan, Oyo State, Nigeria

2 Department of Agricultural and Environmental Engineering, University of Ibadan, Ibadan, Oyo State, Nigeria

3 Department of Geography, University of Ibadan, Ibadan, Oyo State, Nigeria

4 Department of Agricultural and Biosystems Engineering, Kwame Nkrumah University of Science and Technology, PMB, Kumasi, Ghana

5 Centre for Environmental Management, University of the Free State, Bloemfontein 9300, South Africa

Published online: 26 May 2018

previous studies (Ibrahim et al. 2014). Global climate models (GCMs) have coarse resolutions ranging from 1.3° × 1.7° latitude and longitude or 150 × 150 km to 300 × 300 km and therefore require downscaling to finer resolutions depending on the local impact assessments (Gulacha and Mulungu 2016).

Downscaling models have been developed to solve this pending critical aspect of climate assessment (Wigley et al. 1990) resulting from the differences between global and regional climate models as well as local scale assessment. Machenhauer et al. (1996) stated that realistic simulations of the local climate are necessary for meaningful climate change impact studies which GCM does not provide. Downscaling techniques are means of bridging the gap between what climate modelers are able to provide and what impact assessors require (Wilby and Wigley 1997). It interpolates regional-scale atmospheric predictor variables to station-scale meteorological series (Wigley et al. 1990). Regional climate models (RCMs) are nested into GCMs at 50 × 50 km resolution by dynamical downscaling whiles SDSM uses the statistical downscaling approach to generate multivariate regression models in reconstructing data at the point level (Xu 1999; Fowler et al. 2007; Wilby and Dawson 2013; Wilby et al. 2014).

The IPCC Fourth Assessment Report (AR4) on GCMs projects that temperature over West Africa will increase by 1.1–1.3 °C and up to 1.4 °C for the southern and northern regions respectively by 2030 as a result of climate change (WRC 2012). Obuobie et al. (2012) used ECHAM4 and CSIRO with medium resolution to project hotter and dryer climate conditions for the Volta and Pra basins in Ghana. The mean daily temperature was projected to increase by 0.6 and 0.5 °C by 2020 in Volta and Pra basins respectively. They found out that the increase could be as high as 1.9 °C in 2050 at both basins. This projection was relative to the baseline values from 1961 to 1990. It has been found that all models are projecting warming throughout the twenty-first century, at a notable varying details between models (Laprise et al. 2013). The results from the different climate models vary based on resolutions and physical characteristics in boundary conditions of the models. It has been found that the RCMs performance compared to GCMs is not obvious and varies with variables and timescales (Nikiema et al. 2016). Also, the varying resolution amongst RCMs will have the same problems of modeling all variables differently across the regions. Assessing the performance of models helps to identify their capabilities to replicate observed records and determine their level of uncertainties in projections of future variables.

The objective of this study was to project the trends and changes in mean temperature in the Pra River Basin located in the dry sub-humid areas of Ghana for the period 2020–2049 and investigate how variation of model resolution affect efficiency of mean temperature modeling. The five different models grouped into medium (44 km), high (12 km) and very high (2 m) resolutions were used. Statistical Downscaling modeling at very high resolution of 2 m was used to reconstruct observed data with National Centers for Environmental Prediction (NCEP) predictors for the grid boxes of the stations selected and compared with four RCMs in projecting for the period 2020–2049 mean temperature. The spatial distribution of mean temperature for the models were also done.

Data and methodology

Study area

The Pra River Basin has the highest density of settlements (both rural and urban) in Ghana and is located between latitudes 4°58′N and 7°11′N and longitudes 0°25′W and 2°13′W (WRC 2012). It covers an area of 23,321 km^2 extent through almost 55% of Ashanti, 23% of Eastern, 15% of Central and 7% Western Regions (WRC 2012). It has a mean annual discharge of 214 m^3 s^{-1} (Akrasi and Ansa-Asare 2008; WRC 2012). Pra is located in the dry sub-humid region of Ghana (Bizikova 2012) and covered by the moist-semi deciduous forest vegetation which is the largest of the south western drainage basins in Ghana containing most of Ghana's valuable timber trees and cocoa farms (Amisigo et al. 2015). The relative humidity ranges between 60–95% with annual rainfall in the range of 1500–2000 mm. The average maximum and minimum temperatures of the basin are 32 and 21 °C respectively (Akrasi and Ansa-Asare 2008). The largest natural lake in West Africa known as Lake Bosomtwe and some forest reserves like Kakum forest are located in the basin (Fig. 1). The basin was selected for this study because of its response to climate change and the effects on ecosystem deliveries. Pra River Basin is currently the highest spot for tuber crops production in Ghana (Nutsukpo et al. 2013) which may decrease due to the variation of temperature in the area (Brahic 2007; Rasul et al. 2011). The country is also surveying the potential of building a hydro-dam in this basin of which temperature will play a major role in its sustainability (Murphy and Kapelle 2014). Kakum conservation area, which is home to some rare, endangered and vulnerable trees, wildlife, birds and butterfly species is located in the Pra River Basin (IUCN/PACO, 2010).

Data sources

Observed temperature records were acquired from the Ghana Meteorological Agency (GMA). Seven (7) climate stations with data that had limited missing records which could be used were Kumasi Airport, Konongo, Kibi, Akim

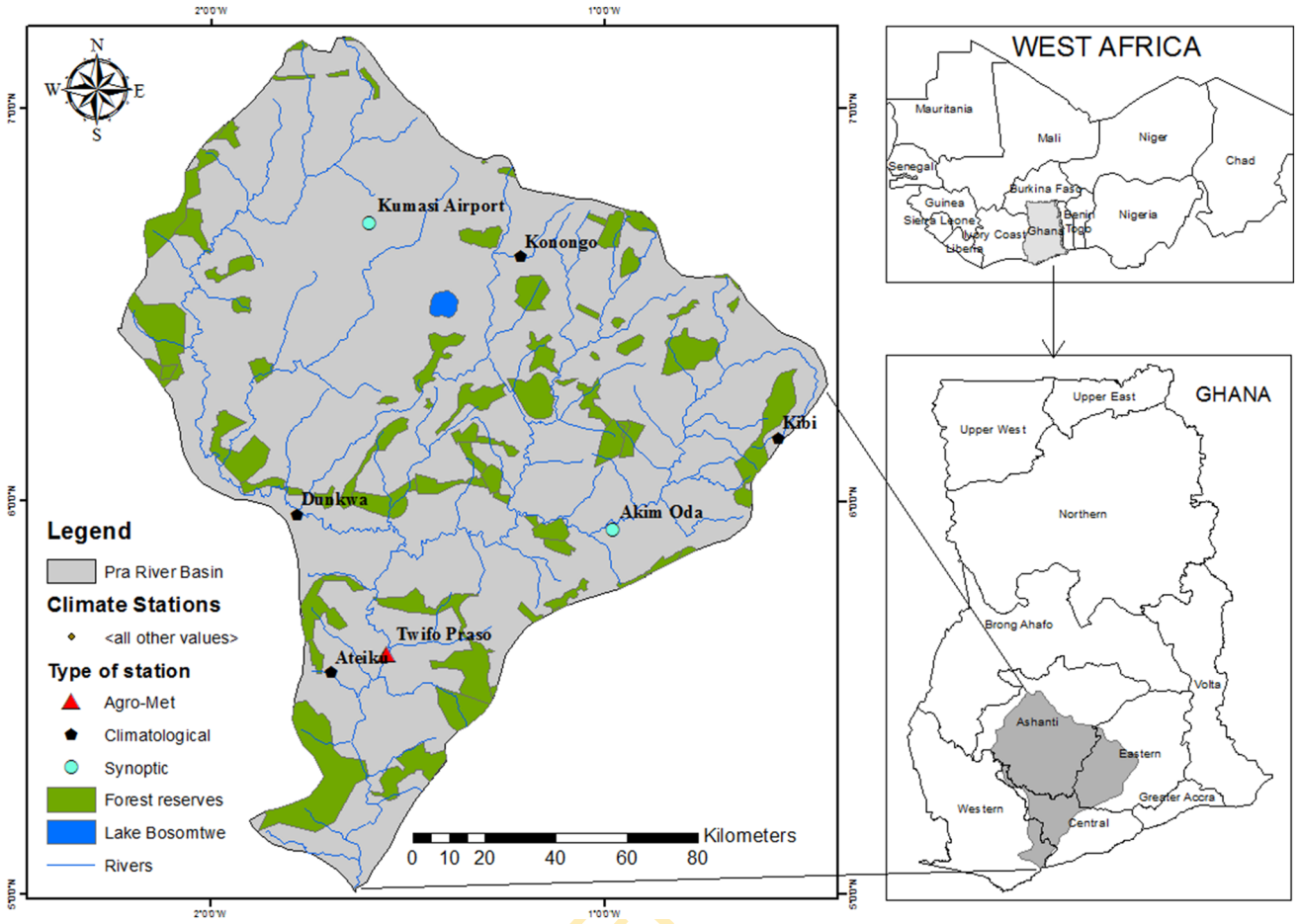

Fig. 1 Map of Pra River Basin

Oda, Dunkwa, Akim Oda, Twifo Praso and Atieku (Fig. 1). The station types were; two synoptic, one agro-meteorological and four climatological stations. The missing data were less than 5% for Kumasi Airport, Konongo, Akim Oda and Dunkwa whereas remaining stations were between 20–50%. Therefore, amelia with four iterations was used in R software to fill the missing data before analysis. The base period years for the performance evaluation of the models was 1980–2010. This was because two of the models from the Weather Research and Forecasting Model (WRF) had a base period from 1980 to 2009 while the remaining three were from 1981 to 2010.

The emission scenario considered for this study was the Representative Concentration Pathways (RCP) 4.5. RCP 4.5 is close to Special Report on Emission Scenarios (SRES) B1 (Clarke et al. 2007; Vuuren et al. 2011; Cubasch et al. 2013). The method of validation of models within acceptable zones of projections (Fenech et al. 2007) was used to select two GCMs from the IPCC fifth Assessment Report (AR5) 43 models. Table 1 shows the full meaning of models abbreviations which will be discussed in preceding paragraphs.

The two GCMs running on SMHI-RCA4 RCM at resolution of 44 km were; CCCma-CanESM2 (hereafter referred to as CanESM) and IPSL-CM5A-MR (hereafter referred to as IPSL). They were acquired from the Coordinated Regional Climate Downscaling Experiment (CORDEX). The other two GCMs running on WRFv3.5.1 model at resolution of 12 km were; GFDL-ESM2M (hereafter referred to as GFDL) and HadGEM2-ES (hereafter referred to as Hadgem). WRF models were also acquired from West African Science Service Centre on Climate Change and Adapted Land Use (WASCAL) geoportal (Heinzeller et al. 2016a, b). The historical simulation of WRF model was from 1980 to 2009. Since the historical simulation of both CORDEX and WRF RCMs ends in 2005, 2006–2010 projections under RCP4.5 run was added to obtain the 1980–2009 and 1981–2010 historical simulation for the evaluation of the performance of the model (Dosio and Panitz 2016). The acquired data from RCMs was mean near-surface air temperature (tas). The fifth model for the study was the Statistical Downscaling Model—Decision Centric (SDSM-DC) version 5.2 (hereafter referred to as SDSM) developed by Wilby and

Table 1 Full description of models

Model code	Full name
CCCma	Canadian Centre for Climate Modeling and Analysis
CanESM2	The second generation Canadian Earth System Model
IPSL	Institut Pierre Simon Laplace
CM5A-MR	Climate Modelling Centre mid-resolution 1.25° × 2.5°
SMHI	Swedish Meteorological and Hydrological Institute
RCA4	Rossby Centre regional atmospheric model
GFDL-ESM2M	The General Fluid Dynamics Laboratory Earth System Model
HadGEM2-ES	Hadley Global Environment Model
WRFv3.5.1	Weather Research and Forecasting Model

Dawson (2013). It was freely acquired from Loughborough University website with the National Centers for Environmental Prediction (NCEP) predictors for calibration (Wilby et al. 2014). The resolution of the SDSM is very high at 2 m. The baseline of 1981–2010 was used because it has a current representation of the present climate compared to 1961–1990 and 1971–2000 climate baseline normal and captures the anthropogenic trends (Arguez et al. 2012). Also, most of the climate stations were active during the selected baseline period which gave minimal missing data (Smith and Pitts 1997; Hulme et al. 1999).

SDSM model calibration and validation

Data for SDSM analysis were prepared in Microsoft Excel 2016 and saved as text file which is the accepted extension of input data in the model. The mean temperature time series was considered an unconditional variable based on its normal distribution. In creating the multivariate regression model in the SDSM software, correlation analysis including correlation matrix and scatter plot were used on all predictors from NCEP in each cell and best correlating independent variables were selected to view their scatter plot graphs. Correlation analysis was done at 0.05 significance and all insignificant and low correlating large scale independent variables were rejected. From the analysis the best predictors for mean temperature are shown in Table 2. The predictors selected for each station were used to calibrate the model. SDSM uses the weather generator to simulate daily data for calibrated variables. Results were extracted into excel via the Time Series Analysis menu. Future climate scenarios were generated using mean factors from the IPCC fifth assessment report (AR5) projections of the various stations which was done using the University of Prince Edward Island (UPEI 2017) Database (https://climate.upei.ca) in Table 5. Since the future period assessment was 2020–2049, the average of 2020s and 2050s validated means was used to generate future scenario at each station. The performance of the model was evaluated with the extracted weather generated results for the base period between 1981 and 2010. The respective coefficient of correlation, r (−) ranged 0.31–0.63 and (+) 0.38–0.70, indicating medium to high performance of the SDSM (Gulacha and Mulungu 2016).

Data analysis

The ncdf.tools, ncdf and raster packages in R software were used to extract grid location specific temperature data from the four RCMs. The performance of the models was evaluated with Nash–Sutcliffe efficiency (NSE), root mean square error (RMSE), and correlation coefficient (R^2) (Moriasi et al. 2007) and areas that models were not within acceptable range of the time-series based metrics were bias-corrected with the variance scaling method using Microsoft Excel

Table 2 The partial correlations between observed station mean temperature at 2 m and selected predictors of model for base period 1981–2010

Predictor	Description	Synoptic Stations						
		Atieku	Dunkwa on Ofin	Twifo Praso	Akim Oda	Kibi	Kumasi	Konongo
lftx	Surface lifted index	−0.49	−0.52	−0.52	−0.51	−0.50		−0.31
mslp	Mean sea level pressure	−0.48	−0.47	−0.51	−0.52	−0.49	−0.63	−0.39
p850	850 hPa geopotential height	−0.32	−0.33	−0.34	−0.36	−0.34	−0.39	
pottmp	Potential temperature	0.50	0.50	0.53	0.54	0.50	0.69	0.38
r500	Relative humidity at 500 hPa height						−0.31	−0.32
shum	Near surface specific humidity	0.63	0.66	0.67	0.67	0.67		
temp	Mean temperature at 2 m	0.54	0.54	0.57	0.58	0.54	0.70	0.49

2016 (Teutschbein and Seibert 2012). The objective of the bias-correction was not to check the effect of bias-correction on model output since it has been done in many other studies (Hashino et al. 2007; Leander et al. 2008; Teutschbein and Seibert 2012; Muerth et al. 2013; Fang et al. 2015; Teng et al. 2015; Jeon et al. 2016) but to correct results of models to improve the accuracy of ensemble projection from this study. The climate extreme indices were also determined using Instat v3.36 software (New et al. 2006). Model results were transferred into ArcGIS 10.4 and kriging method was used to generate the temperature maps of the basin for the period 2020–2049.

Performance evaluation of models

It is paramount to check performance of the models in simulating current climate before accepting the credibility of model projections (Laprise et al. 2013). GFDL and Hadgem were biased corrected for all stations except Kumasi where only GFDL data needed bias-correction. CanESM output was good for three out of four stations that needed no bias-correction whiles IPSL was okay for only two stations (Dunkwa and Kumasi) as shown in Table 3. NSE were very good for all models (both bias-corrected and those that needed no bias-correction) except the IPSL at Dunkwa which was very low (0.04) but was still within the range of acceptable models (Table 3). RMSE ranged between 0 and 0.97. Studies have shown that the lower the RMSE the better the model, therefore both the unbiased and bias-corrected models used in this study are within acceptable limits (Moriasi et al. 2007). All bias-corrected models were not in acceptable levels of performance with observed data before variance scaling method of bias-correction was applied (Teutschbein and Seibert 2012). From the performance evaluation, SDSM was the best amongst the five to model mean temperature in the Pra River Basin followed by CanESM which had three out of seven stations within acceptable levels of modeling without bias-correction. Although IPSL was not as good as the first two, it was better than Hadgem and GFDL in order of descending in efficient modeling of mean temperature over the study area.

Results and discussion

Historical temperature trend in the basin

Maximum temperature varied widely with about 29.8 °C at Konongo in 1999 to 33 °C at Twifo Praso in 1997. The mean maximum temperature ranged between 31.04–32.15 °C with an increasing trend from 1981 to 2010 (Fig. 2). Maximum temperature increased by 1.11 °C within this period with hottest peaks in 1983, 1987, 1995 and 1998. The lowest minimum temperature of about 19.3 °C was recorded in Konongo in 1999 while Twifo Praso recorded the highest minimum temperature of about 23.3 °C in the year 2010. The mean minimum temperature varied between 21 and 22.47 °C (Fig. 2) indicating temperature rise of 1.47 °C within the assessed period. This finding confirms the temperature range of the Pra River Basin which has been reported to

Table 3 Nash–Sutcliffe efficiency (NSE), Root-mean-square error (RMSE) and coefficient of determination (R^2) for comparison of observed period and model historical monthly mean

	Ateiku	Akim Oda	Dunkwa	Kibi	Konongo	Kumasi	Twifo Praso
Nash–Sutcliffe efficiency (NSE)							
SDSM	0.99	0.99	0.99	0.99	0.99	0.99	0.99
CanESM	1[a]	1[a]	0.52	1[a]	1[a]	0.83	0.28
IPSL	1[a]	1[a]	0.04	1[a]	1[a]	0.44	1[a]
Hadgem	0.99[a]	1[a]	1[a]	1[a]	1[a]	0.12	1[a]
GFDL	0.99[a]	1[a]	1[a]	1[a]	1[a]	1[a]	1[a]
Root mean square error (RMSE)							
SDSM	0.01	0.03	0.02	0.01	0.01	0.03	0.02
CanESM	0.0002[a]	0.0003[a]	0.55	0.0002[a]	0.0003[a]	0.37	0.63
IPSL	0.0003[a]	0.0003[a]	0.73	0.0003[a]	0.0005[a]	0.62	0.0004[a]
Hadgem	0.0004[a]	0.00011[a]	0.0009[a]	0.0006[a]	0.0008[a]	0.97	0.0006[a]
GFDL	0.014[a]	0.0009[a]	0.0009[a]	0.0005[a]	0.0005[a]	0.0009[a]	0.0008[a]
Coefficient of determination (R^2)							
SDSM	0.99	0.99	0.99	0.99	0.99	0.99	0.99
CanESM	1[a]	1[a]	0.91	1[a]	1[a]	0.91	0.89
IPSL	1[a]	1[a]	0.93	1[a]	1[a]	0.86	1[a]
Hadgem	0.99[a]	1[a]	1[a]	1[a]	1[a]	0.68	1[a]
GFDL	0.99[a]	1[a]	1[a]	1[a]	1[a]	1[a]	1[a]

[a]Bias corrected with variance scaling method

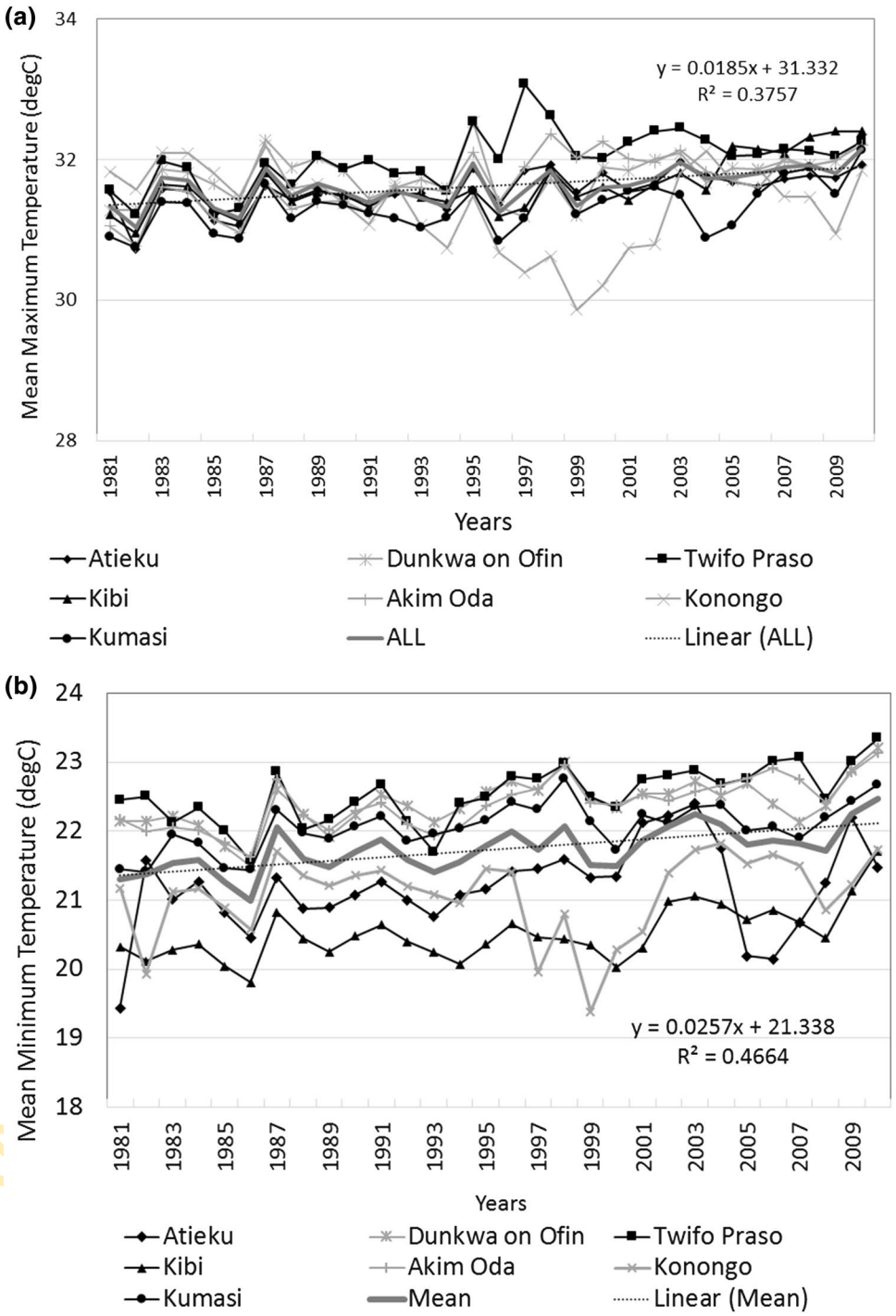

Fig. 2 Observed temperature trends in the Pra River Basin: **a** maximum and **b** minimum

be between 21 and 32 °C by previous studies (Akrasi and Ansa-Asare 2008). The increasing trend in mean maximum (+1.11 °C) and mean minimum (+1.47 °C) temperature shows that minimum temperature is increasing faster than maximum temperature. This finding was similar to Kima et al. (2015) who found maximum and minimum temperature between 1980 and 2012 to have increased by +0.66 and +0.89 °C in the sub-humid zone of Burkina Faso. It implies that temperature change is higher in the dry sub-humid zone of Ghana than the sub-humid zone of Burkina Faso. Other studies in the region also confirms that minimum temperature is increasing faster than maximum temperature (Vose et al. 2005).

The increasing temperature trends in the Pra River Basin varied from one station to another. The highest mean temperature for the base period 1981–2010 and 1980–2009 were recorded at Twifo Praso at 27.3 and 27.14 °C respectively while Kibi station recorded lowest mean temperature of the

base periods. Both 1981–2010 and 1980–2009 recorded 26.1 °C for Kibi station. Increased greenhouse gases in the atmosphere forms an atmospheric canopy that reduce the amount of heat leaving the earth surface popularly known as the greenhouse effect (IPCC 1990, 2007; Anderson et al. 2016). Therefore, daily insolation increases the amount of heat on earth leading to the recorded rise in temperature. Climate change has been found to increase cloudiness and therefore leading to higher albedo percentage with negative effect on global warming (Held and Soden 2000). It is likely that albedo effect of increased clouds due to the amount of water vapour in the atmosphere during the daytime reduces the rate of maximum temperature rise compared to the nighttime when even heat from earth surface is limited by greenhouse effect (Karl et al. 1993; Anderson et al. 2016; Oktyabrskiy 2016). Also urban heat island is strongest in the nighttime hours which contributes to the quick rise in minimum temperature in the Pra River Basin as the rate of urbanization cannot be ignored (Karl et al. 1993, 1999; GSS 2014).

The climate extreme temperature indices showed that frequency of cool day (< 28.7 °C) and warm day (> 34.3 °C) were 8.37 and 7.95% respectively. There were more cool days than warm days in the observed period of 1981–2010 in the basin. Also, cool night (< 20.13 °C) and warm night (> 23.41 °C) frequency were at 6.83 and 4.66% respectively (Table 4). These findings were about 1.7–5% lower than the extreme temperature occurrence in the sub-humid regions of Burkina Faso (Ly et al. 2013; Kima et al. 2015). The counts of cool days were more than warm days which further explains the slow rate of rising maximum temperature attributed to cloudiness and albedo negative effective on global warming (Held and Soden 2000). Pollination which is an important stage in crop production is very sensitive to temperature extremes (Hatfield and Prueger 2015) that led to inconsistency in crop production in the basin in the last decade of baseline period (Nutsukpo et al. 2013). There were more cool nights than warm ones in this period accounting for more stable production than irregularities since respiration in crop growth is less sensitive to night temperatures (Frantz et al. 2004).

IPCC AR5 temperature projections over Pra River Basin

An area between latitude 4.94 N and 7.20 N and longitude 0.95 W and 2.65 W was selected on the UPEI database using scatter plot analysis for temperature covering an area of 47, 192 km^2. Mean temperature which is the ensemble of all 43 models was 26.30 °C with maximum and minimum of 28.36 and 24.64 °C respectively for the base period 1981–2010. The result was very close to the mean of the seven stations which was 26.33 °C (Table 5).

Table 4 Extreme temperature indices for 1981–2010 in the Pra River Basin

Index	Descriptive names	Definition	Value
TxMean	Mean annual maximum temperature		31.62 (2.12) °C
TnMean	Mean annual minimum temperature		21.74 (1.57) °C
Tx10P	Cool day frequency	Percentage of days with TX < 10th percentile of data	8.37%
Tx90P	Warm day frequency	Percentage of days with TX > 90th percentile of data	7.95%
Tn10P	Cool night frequency	Percentage of days with TN < 10th percentile of data	6.83%
Tn90P	Warm night frequency	Percentage of days with TN > 90th percentile of data	4.66%

Table 5 AR5 ensemble and validated temperature projections in the Pra River Basin

Climate stations	Ensemble (mean)				Validated mean			
	Baseline (°C)	2020s (°C)	2050s (°C)	2080s (°C)	Baseline (°C)	2020s (°C)	2050s (°C)	2080s (°C)
Akim Oda	26.25	0.83	1.76	2.68	25.98	0.91	1.91	2.88
Kumasi	25.94	0.84	1.79	2.74	25.31	0.95	1.95	2.98
Atieku	26.84	0.72	1.52	2.31	26.20	0.72	1.53	2.33
Dunkwa on Offin	26.18	0.84	1.77	2.69	25.58	0.91	1.83	2.79
Twifo Praso	26.72	0.78	1.65	2.51	25.88	0.79	1.67	2.54
Kibi	26.38	0.83	1.77	2.70	25.54	0.92	1.90	2.86
Konongo	26.00	0.84	1.79	2.73	25.46	0.93	1.96	3.02
Mean	26.33	0.81	1.72	2.62	25.71	0.88	1.82	2.77

Ensemble—average of all 43 AR5 GCMs. Validated—models with acceptable performance over the study area

The mean of the model was 0.37 °C below the actual mean of the observed calculated data of 26.70 °C. The ensemble of GCMs projected temperature change of +0.80, +1.68 and +2.56 °C for the future period of 2020s (2011–2040), 2050s (2041–2070) and 2080s (2071–2100) respectively are presented in Fig. 3. This is comparable to the Earth system version of the Canadian Centre for Climate Modelling and Analysis (CanESM2) and the Earth system version of the Max Planck-Institut fur Meteorologie (MPI-ESM-LR) GCMs projection over the southern part of Ghana by Laprise et al. (2013). CanESM2 projected 0.5–1.5 and 1.5–3 °C for January–February–March (JFM) for the period 2020s and 2050s respectively. This projection of JFM reduced in July–August–September (JAS) which was 0.5–1 and 1–2 °C for same future periods. It implies that the IPCC AR5 projections of the 43 ensemble for the Pra River Basin is within the range of modelled results over southern Ghana (Laprise et al. 2013). MPI-ESM-LR projected the range of 0.5–1 °C mean temperature change for same location for both JFM and JAS for the period 2020s and increased temperature change of 1.5–2 °C for JFM and 1–1.5 °C for JAS in 2050s. Maximum temperature change is projected to increase as high as 5 °C in 2100 while minimum temperature change will be around 0.8 °C. However, spatial temperature change projections over the basin was 0.1–0.6 °C lower than the mean of the selected stations (Table 5). This might be attributed to the rectangular box selection of coordinates which expand beyond the basin to other basin especially at the southern part of Pra River Basin due to its reduced size. Validation results which is calculated as the average of the models within acceptable range of first standard deviation was 0.62 °C lower than the mean of ensemble as shown in Table 5. Under the 2020s projection of +0.80 °C, climate related diseases will increase and more warm nights will be experienced (Brahic 2007; Obuobie et al. 2012). The +1.68 °C temperature increase in the 2050s is likely to reduce crop yield, increase the rate of malaria infections and reduce water yield in the basin. Cocoa and other cash crop production will be more vulnerable to the attack of pest that are emerging because of increasing temperature in the basin. Army worms and other cereal crops pest may also increase and reduce yield (Brahic 2007; Hatfield and Prueger 2015). This will definitely affect the livelihood of the dwellers since majority are farmers (GSS 2014). The 2080s projection of +2.56 °C will aggravate the situation of water scarcity, low crop yield, floods and droughts, poverty and malnutrition and possibly lead to migration (Brahic 2007; Obuobie et al. 2012; Nutsukpo et al. 2013). Within the projected change of +0.80 to +2.56 °C, soil temperature will also increase affecting root development directly in their nutrient uptake and respiration processes (IPCC 2014; Gray and Brady 2016).

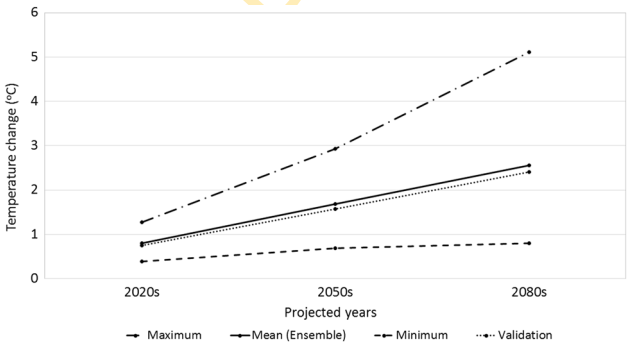

Fig. 3 Projections of future temperature change over Pra river basin

Projected trends of near future mean temperature

The mean historical temperature of SDSM, CanESM and IPSL for the base period 1981–2010 were 26.71, 26.72 and 26.79 °C, showing a deviation of +0.01, +0.02 and +0.09 °C respectively from the observed data in the Pra River Basin. Comparing the mean temperature output of Hadgem and GFDL to the observed records of the basin between 1980 and 2009 (26.56 °C), GFDL modelled 0.10 °C more whiles Hadgem modelled 0.01 °C less.

The mean temperature projections for 2020–2049 were 28.04, 28.04, 28.15, 27.74 and 27.62 °C for SDSM, CanESM, IPSL, Hadgem and GFDL respectively. Analysis of variance (ANOVA) at 95% confidence indicated that there is a significant difference between the mean temperature of the five models for the projected period ($p = 2.086 \times 10^{-12}$). However, ANOVA of SDSM, CanESM and IPSL indicated no significant difference in the mean temperature of projections ($p = 0.252$). Also, there was no significant difference between Hadgem and GFDL ($p = 0.1062$). It implies that resolution of models affects their output but in this case, SDSM at resolution 2 m is not different from CanESM and IPSL at resolution of 44 km. This could be due to the effectiveness and efficiency of the RCMs at that medium resolution to capture the temperature conditions of the basin better than WRF models. All models correlated positively under the Pearson correlation (R) with SDSM and CanESM having the highest correlation at $R = 0.727$ and the lowest between IPSL and CanESM at $R = 0.366$. Pearson correlation measures the strength of the linear relationship between two variables as they vary in time (Nikiema et al. 2016).

From Fig. 4, all models projected an increasing trend in mean temperature for the period (2020–2049). CanESM projected hottest years of 28.14, 28.21, 28.65 and 28.59 °C mean temperature for 2021, 2030, 2037 and 2041 respectively. The temperature peaks indicating hottest years varied from one model to another. IPSL projected 2025, 2034, 2044 and 2047 as hottest years with mean temperature at 28.35, 28.69, 28.62 and 28.75 °C respectively. GFDL projected

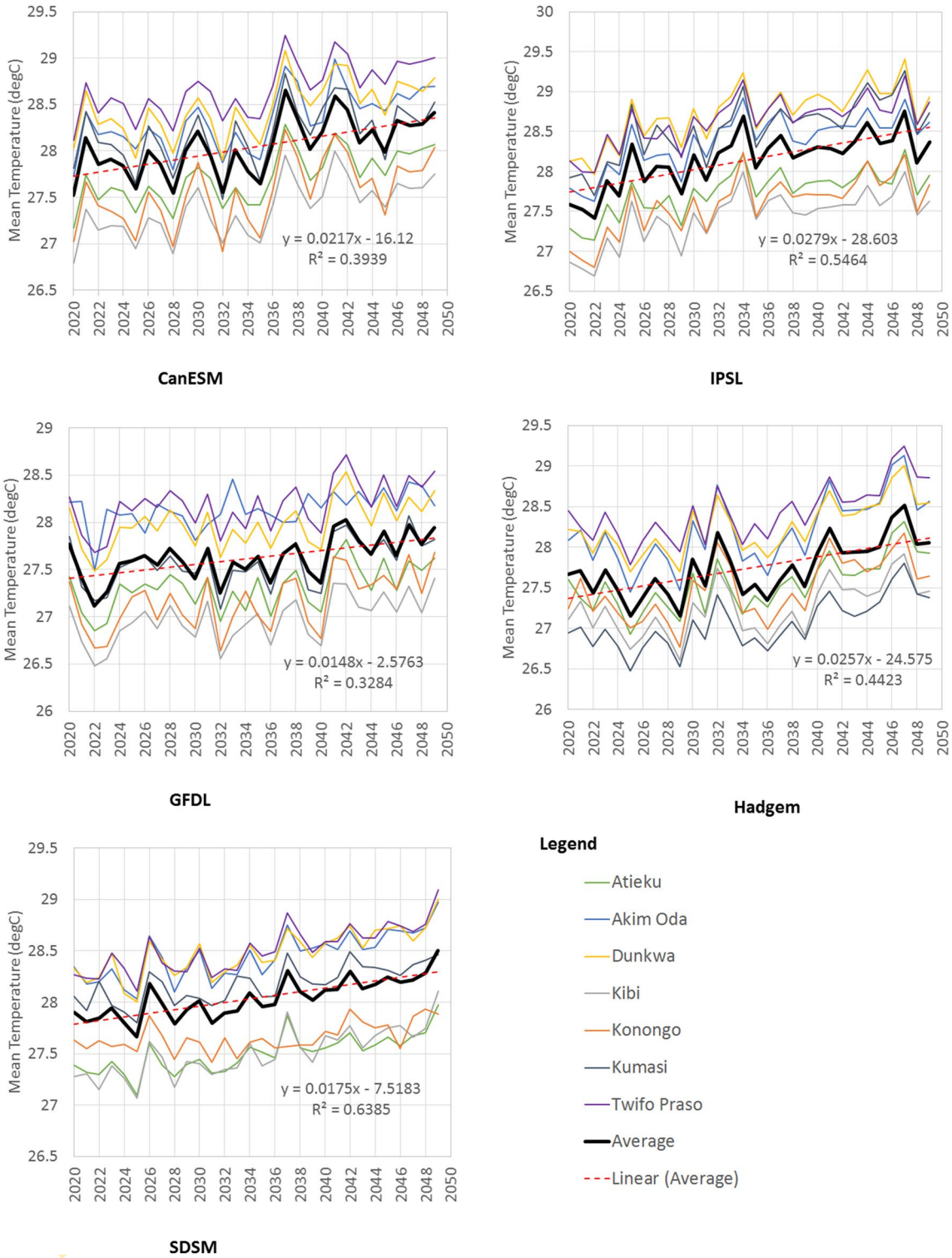

Fig. 4 Projected mean temperature by the five models

only one major peak in 2042 at 28.02 °C whereas Hadgem in same resolution projected 2032, 2041 and 2047 to be hottest with mean temperature of 28.18, 28.23 and 28.51 °C respectively. SDSM also indicated that 2026, 2037, 2042 and 2049 will be hottest at mean temperature of 28.18, 28.31, 28.30 and 28.50 °C respectively (Fig. 4). Twifo Praso was projected with the highest temperature for all models except at IPSL which was Dunkwa station whiles Kibi was

the lowest from all except SDSM and Hadgem that project Atieku and Kumasi stations to be lowest. The hottest years or peaks projected by the five models agree with the maximum temperature projection of the AR5 43 GCMs for the basin which was determined to be 28.36 °C for the base period 1981–2010 (Table 5). This implies that the maximum of the base period from AR5 assessment and mean maximum temperature of the historical period 1981–2010 may become the mean temperature in the future period. Extreme events of temperature resulting in heat shock [short period of very high temperatures (> 33 °C)] has a significant risk impact on crop production (Barlow et al. 2015). Kumasi which is the second highest growing city in Ghana is located in the basin. This urban population being fed by migrations from surrounding regions like Central and Eastern regions of Ghana with a net volume of migration of − 274,579 and − 224,386 in 2000 and − 238,015 and − 332,086 in 2010 respectively (GSS 2014) will contribute to increased urban heat island (Karl et al. 1993). The years 2041, 2042 and 2047 were projected by minimum of two different models as hottest years to have mean temperature peaks of averagely 28.41, 28.16 and 28.63 °C respectively. The rare and endangered species of wildlife, consisting of 226 bird species and minimum of 405 butterfly species habiting the Kakum conservation area in the basin will be exposed to increased temperature that might cause some to migrate and less resilient ones to even be extinct from the park (UICN/PACO 2010; Dowsett-Lemaire and Dowsett 2011). The already polluted rivers in the Pra River Basin (Ansa-Asare et al. 2014) combined with increased stream temperature resulting from the projected temperature change will also change the stream chemistry and play a critical role in the fluvial erosion of cohesive streambanks (Hoomehr et al. 2018).

The monthly distribution of mean temperature in the basin for the observed period 1981–2010, varied with August recording the lowest at 25.21 °C and March recording the highest at 28.04 °C. Seasonal variation was also seen between February–April and July–September where the former recorded high mean temperature and the latter was the lowest for the observed period (Fig. 5). The ensemble of the five models for the period 2020–2049, depicted same trend of February–April as high and July–September as the lowest in the future similar to the findings that June to September/October is a cooler period in the basin (Akrasi and Ansa-Asare 2008). However, January is projected to have the highest change in mean temperature of + 1.51 °C. From Fig. 5, the secondary axis shows the mean temperature change projected by the five models used in this study. The mean temperature change was projected at 1.37, 1.47, 1.06, 1.18 and 1.36 °C by CanESM, IPSL, GFDL, Hadgem and SDSM respectively. The lowest temperature change was projected by GFDL at 0.35 °C in January and highest at 2.30 °C in December by Hadgem. All models projected

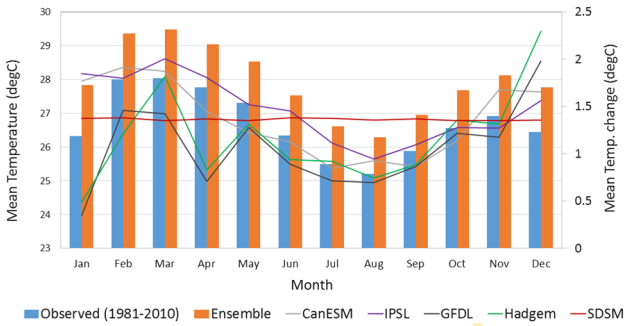

Fig. 5 Monthly distribution of observed and future (2020–2049) ensemble mean temperature (primary axis) and mean temperature changes (secondary axis) of the five models

mean temperature change trend to drop from June to August and rise from August to October except SDSM which was even around 1.36 °C for those 5 months (Fig. 5). Contrary to the findings of Laprise et al. (2013) that mean temperature change of JAS season is generally warmer than JFM, JFM in the Pra River Basin is projected to be higher than JAS for all models. It is worth noting that mean temperature in the dry season from December to February is not as high as from February to April. This might be due to the harmattan which occurs from December to February in the study location. Evaporation is expected to increase from February to April thereby extending the dry periods of the basin from December to April. This dry period may result in rainfall deficits which will affect the development of crops in the first raining season, hence having an impact on farmers who are engaged solely in rainfed agriculture.

Spatial distribution of future mean temperature in the basin

Temperature change across the stations projected for the period 2020–2049 were all positive and varied between 0.40–1.49 °C amongst the five models (Table 6). This was similar to the AR5 ensemble projected temperature change of 0.80 and 1.68 °C for the period 2020s and 2050s respectively. It implies that the models are within the global climate projections for the basin. Hadgem projected the lowest change and both SDSM and CanESM projected the highest change of same value. Both changes in projections were at Kumasi Airport (Table 6).

The ensemble results of this study confirm the IPCC AR4 temperature projection over West Africa to increase by 1.1–1.3 °C in 2030 (WRC 2012). Only the Hadgem projection at Kumasi Airport station was close to the 2020s (2011–2040) temperature change results from ECHAM4 and CSIRO joint model for the Pra River Basin which was at 0.5 °C (Obuobie et al. 2012). GFDL projections were all below increase of 1 °C except at Akim Oda stations which

Table 6 Projected changes in temperature (°C) in 2020–2049

Model	Atieku	Akim Oda	Dunkwa	Kibi	Konongo	Kumasi	Twifo Praso
CanESM	1.34	1.30	1.37	1.31	1.34	1.49	1.40
IPSL	1.37	1.35	1.63	1.36	1.38	1.84	1.37
GFDL	0.93	1.14	0.94	0.94	0.97	0.92	0.94
Hadgem	1.17	1.21	1.20	1.20	1.28	0.40	1.18
SDSM	1.12	1.41	1.39	1.44	1.45	1.49	1.25
Ensemble	1.19	1.28	1.31	1.25	1.28	1.23	1.23

was 1.14 °C. Spatially, SDSM, CanESM and IPSL showed a good distribution of temperature change in the basin with increasing change from the south to the north in the case of SDSM and from south-east upwards for CanESM and IPSL (Fig. 6). It could be seen that the low projection of change at Kumasi by Hadgem and GFDL affected the ensemble map significantly. Temperature change distribution was between 1.15–1.48 °C for SDSM, 1.31–1.46 °C for CanESM, 1.38–1.68 °C for IPSL, 0.92–1.14 °C for GFDL and 0.41–1.28 °C for Hadgem.

Generally, temperature increases northward in Ghana (Nutsukpo et al. 2013) which is depicted accurately by the SDSM map. Kumasi Metropolitan Assembly, the largest and most industrious city in the whole basin was mapped by CanESM, SDSM and IPSL to have the highest temperature change in the period 2020–2049. This was contrary to the projection of the WRF models (Hadgem and GFDL) which mapped same Assembly as the lowest temperature change location. Studies have shown that temperature change in urban industrious areas are higher compared to other location with less industrial activities. Also, population has been found to have a direct effect on the atmospheric temperature in the immediate environment due to urban heat island effect (Sakakibara and Owa 2005; Zielinski 2014; Zeleňákováa et al. 2015). The temperature distribution in Ghana becomes hotter as you move from the south to north of the country. Therefore, SDSM, CanESM and IPSL (RCA4) was a better model to predict temperature trend in the basin compared to Hadgem and GFDL from the WRF-model which has 12 km resolution.

Implication of projected temperature trends in the basin

Higher night temperatures increase respiration in crops which stress plants thereby reducing the net gain in the form of grain yield. Temperature rise causes significant reduction in grain yield and affect the health of crops especially during the reproductive stage of crops life cycle. Increased temperature affects the physiological processes necessary for crop growth and development which leads to drop in crop yields. Temperature anomalies is playing an important role in the uncertainties of crop production in this century (Rasul et al. 2011). Crop yields in Africa is estimated to drop by 5–10% at 2 °C temperature rise (Brahic 2007). The reproductive stage of development of cereals such as maize is primarily impacted by warmer temperatures with a significant reduction in grain yield (Hatfield and Prueger 2015).

Water availability in some vulnerable regions such as Africa has been estimated to decrease between 20 and 30% at 2 °C rise in temperature (Brahic 2007). Increasing temperature trends will also affect the annual flow of the basin negatively since temperature increase will also lead to evaporation increase and might results in droughts (Murphy and Charlton 2006; Arias et al. 2014; Gulacha and Mulungu 2016). Elderd and Reilly (2014) reported that disease transmission and outbreak intensity increased at higher temperatures. This was done by measuring the cumulative fraction infected during an epizootic although the change in mean transmission rate was not appreciable. Also, it has been found that a rise in atmospheric temperature tend to increase most diseases (Choi et al. 2007). For instance, about 40–60 million people have been estimated to be exposed to malaria in Africa by 2 °C increase in temperature (Brahic 2007). Increasing temperature trends in the basin will increase the release of carbon and methane through increased rate of root respiration that could significantly affect soil processes like decomposition and water transportation. Crowther et al. (2016) reported that 1 °C temperature rise will result in the release of 30 petagrams of carbon. Therefore, the average increase of 1.25 °C for the future period 2020–2049 is expected to emit more carbon dioxide than the base period.

Conclusion

Findings from the study indicate that mean minimum temperature is increasing faster than maximum mean temperature for the observed period between 1981 and 2010 which might explain the increased warming experienced in the night across the country. The best models after performance evaluation deviated from their base period by +0.01, +0.02 and +0.09 °C for SDSM, CanESM and IPSL respectively. SDSM has a resolution of 2 m whereas CanESM and IPSL from RCA4 are at a resolution of 44 km but their outputs

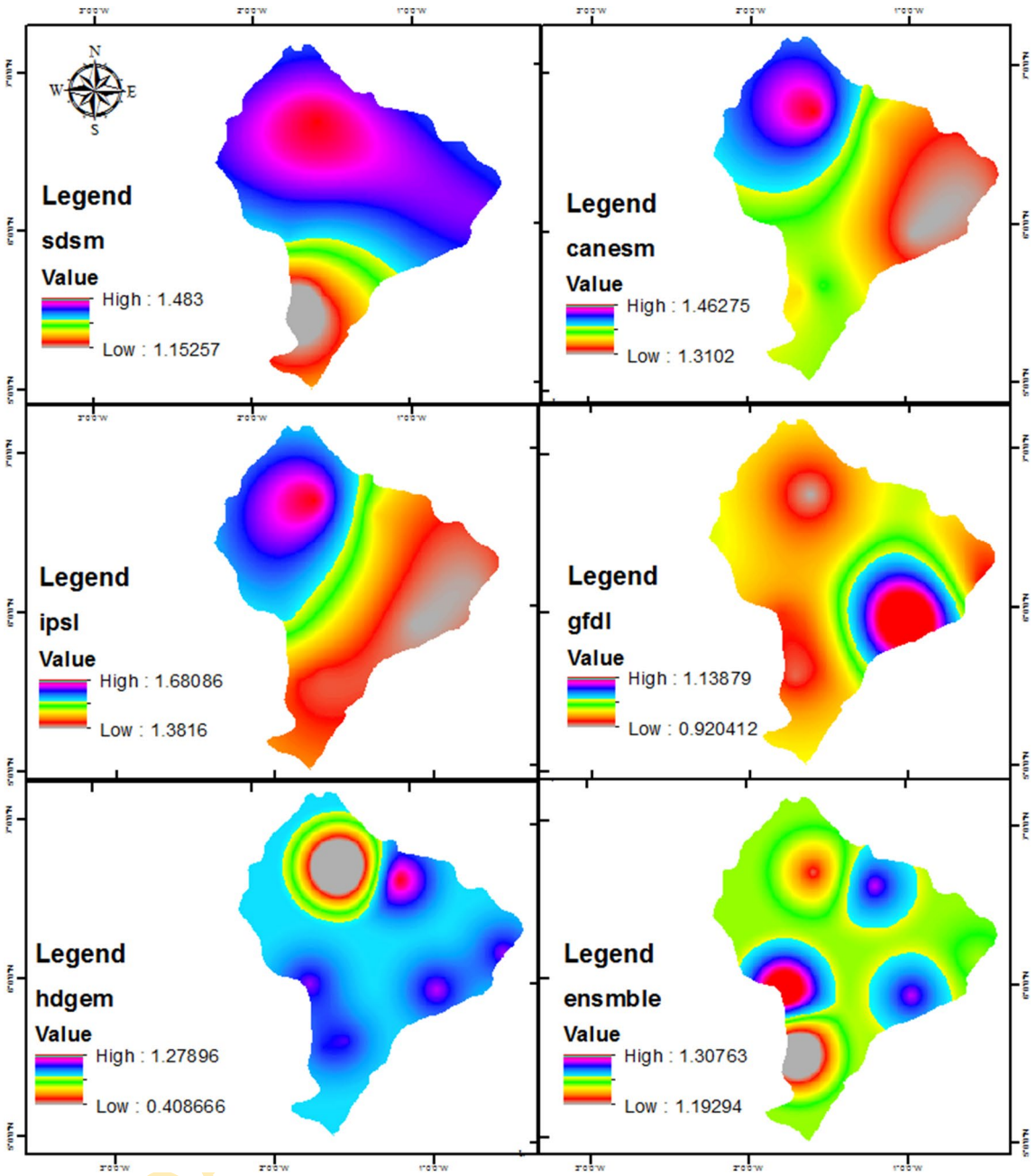

Fig. 6 Spatial model projection of future temperature change by kriging

are better and correlate very well compared to WRF models which were at resolution of 12 km. Although resolution of models affects its accuracy, this result shows that, the setting of good boundary conditions to replicate the predictors influencing the climate of a particular area in RCMs has a possibility of affecting the efficiency of the model's performance. That's why CORDEX RCMs at 44 km performed better than WRF in this study. There was an increasing trend of mean temperature by all models in the period 2020–2049 with the years 2041, 2042 and 2047 identified as hottest at mean temperature peaks of 28.41, 28.16 and 28.63 °C, respectively. Projected temperature change may reduce crop yield by increasing plant respiration and affecting other physiological processes at the development stage. Evaporation will also increase thereby reducing annual river flows which may results in droughts. Rate of soil carbon loss will be increased by the increasing temperature change projected and diseases like malaria is also estimated to rise. Appropriate adaptation strategies are recommended to be practiced by farmers and residents in order to curb the impact of rising temperature in

the basin as a results of climate change. Also, measures must be put in place by health services to control the projected spread of climate related diseases like malaria in order to protect basin dwellers from climate related disease mortality. Both plant and animal species within the protected areas in the basin will require the strict implementation of effective reserve management practices to conserve the rare and endangers species seeking habitat in the basin.

Acknowledgements This paper was extracted from Ph.D. thesis to be submitted to the Pan African University Institute of Life and Earth Sciences at the University of Ibadan, Nigeria funded by the African Union Commission. Maximum and minimum temperature data were acquired from the Ghana Meteorological Agency with great appreciation. Authors also appreciate, http://climate4impact.eu, West Africa Science Service Center on Climate Change and Adapted Land Use (WASCAL) Geoportal and http://co-public.lboro.ac.uk websites and hosts for free access downloads of CCCma-CanESM2 and IPSL-CM5A-MR (CORDEX models), GFDL-ESM2M and HadGEM2-ES (WRF models) and SDSM-DC model respectively. We are also grateful to University of Prince Edward Island (UPEI) for access to their climate Database for fifth assessment report GCMs analysis in this study.

References

Akrasi SA, Ansa-Asare OD (2008) Assessing sediment and nutrient transport in the Pra Basin of Ghana. West Afr J Appl Ecol 13:45–54. https://doi.org/10.4314/wajae.v13i1.40583

Amisigo BA, McCluskey A, Swanson R (2015) Modeling impact of climate change on water resources and agriculture demand in the Volta Basin and other Basin Systems in Ghana. Sustainability 7:6957–6975. https://doi.org/10.3390/su7066957

Anderson TR, Hawkins E, Jones PD (2016) CO_2, the greenhouse effect and global warming: from the pioneering work of Arrhenius and Callendar to today's Earth System Models. Endeavour 40(3):178–187. https://doi.org/10.1016/j.endeavour.2016.07.002

Ansa-Asare OD, Entsua-Mensah RE, Duah AA, Owusu BK, Amisigo B, Mainoo PK, Obiri S (2014) Multivariate and spatial assessment of water quality of the Lower Pra basin, Ghana. J Nat Sci Res 4(21):99–113

Arguez AI, Durre S, Applequist RS, Vose MF, Squires X, Yin RR, Heim Jr, Owen TW (2012) NOAA's 1981–2010 U.S. Climate Normals: an overview. Bull Am Meteorol Soc 93:1687–1697. https://doi.org/10.1175/BAMS-D-11-00197.1

Arias R, Rodríguez-Blanco ML, Taboada-Castro MM, Nunes JP, Keizer JJ, Taboada-Castro MT (2014) Water resources response to changes in temperature, rainfall and CO_2 concentration: a first approach in NW Spain. Water 6:3049–3067. https://doi.org/10.3390/w6103049

Barlow KM, Christy BP, O'Leary GJ, Riffkin PA, Nuttall JG (2015) Simulating the impact of extreme heat and frost events on wheat crop production: a review. Field Crops Res 171:109–119. https://doi.org/10.1016/j.fcr.2014.11.010

Bizikova L (2012) Semi-arid areas. Collaborative Adaptation Research Initiative in Africa and Asia Presentation at Doha Climate Change Conference, COP 18. https://www.idrc.ca/sites/default/files/sp/...CARIAA_COP18_Policy_Semi-arid.pdf. Accessed 30 Dec 2017

Brahic C (2007) The impacts of rising global temperatures. Daily News 2. https://www.newscientist.com/article/dn11089-the-impacts-of-rising-global-temperatures/. Accessed 8 Jan 2018

Choi SH, Lee SW, Hong YS, Kim SJ, Kim NH (2007) Effects of atmospheric temperature and humidity on outbreak of diseases. Emerg Med Australas 19(6):501–508. https://doi.org/10.1111/j.1742-6723.2007.01000.x

Clarke L, Edmonds J, Jacoby H, Pitcher H, Reilly J, Richels R (2007) Scenarios of greenhouse gas emissions and atmospheric concentrations. Sub-report 2.1A of Synthesis and Assessment Product 2.1 by the U.S. Climate Change Science Program and the Subcommittee on Global Change Research. Office of Biological and Environmental Research, Washington DC, p 154

Crowther TW, Todd-Brown KEO, Rowe CW, Wieder WR, Carey JC, Machmuller MB, Snoek BL, Fang S, Zhou G, Allison SD, Blair JM, Bridgham SD, Burton AJ, Carrillo Y, Reich PB, Clark JS, Classen AT, Dijkstra FA, Elberling B, Emmett BA, Estiarte M, Frey SD, Guo J, Harte J, Jiang L, Johnson BR, Kröel-Dulay G, Larsen KS, Laudon H, Lavallee JM, Luo Y, Lupascu M, Ma LN, Marhan S, Michelsen A, Mohan J, Niu S, Pendall E, Peñuelas J, Pfeifer-Meister L, Poll C, Reinsch S, Reynolds LL, Schmidt IK, Sistla S, Soko NW, Templer PH, Treseder KK, Welker JM, Bradford MA (2016) Quantifying global soil carbon losses in response to warming. Nature 540:104–110. https://doi.org/10.1038/nature20150

Cubasch U, Wuebbles D, Chen D, Facchini MC, Frame D, Mahowald N, Winther J-G (2013) Introduction. In: Stocker TF, Qin D, Plattner G-K, Tignor M, Allen SK, Boschung J, Nauels A, Xia Y, Bex V, Midgley PM (eds) Climate Change 2013: the physical science basis. Contribution of Working Group I to the Fifth Assessment Report of the Intergovernmental Panel on Climate Change. Cambridge University Press, Cambridge, pp 119–158

Dosio A, Panitz H-J (2016) Climate change projections for CORDEX-Africa with COSMO-CLM regional climate model and differences with the driving global climate models. Clim Dyn 46:1599–1625. https://doi.org/10.1007/s00382-015-2664-4

Dowsett-Lemaire F, Dowsett RJ (2011) An update on the birds of Kakum National Park and Assin Atandaso Resource Reserve, Ghana. A report prepared for the Wildlife Division, Forestry Commission, Accra. Dowsett-Lemaire Misc. Report 75

Elderd BD, Reilly JR (2014) Warmer temperatures increase disease transmission and outbreak intensity in a host-pathogen system. J Anim Ecol 83(4):838–849. https://doi.org/10.1111/1365-2656.12180

Fang GH, Yang J, Chen YN, Zammit C (2015) Comparing bias correction methods in downscaling meteorological variables for a hydrologic impact study in an arid area in China. Hydrol Earth Syst Sci 19:2547–2559. https://doi.org/10.5194/hess-19-2547-2015

Fenech A, Comer N, Gough W (2007) Selecting a global climate model for understanding future scenarios of climate change. In: Fenech A, MacLellan J (eds) Linking climate models to policy and decision-making. Environment Canada, Toronto, pp 133–145

Fowler HJ, Blenkinsopa S, Tebaldib C (2007) Review: linking climate change modelling to impacts studies: recent advances in downscaling techniques for hydrological modelling. Int J Climatol 27:1547–1578

Frantz JM, Cometti NN, Bugbee B (2004) Night temperature has a minimal effect on respiration and growth in rapidly growing plants. Ann Bot 94(1):155–166. https://doi.org/10.1093/aob/mch122

Gray SB, Brady SM (2016) Plant developmental responses to climate change. Dev Biol 419:64–77. https://doi.org/10.1016/j.ydbio.2016.07.023

GSS (2014) 2010 Population and Housing Census Report: urbanization. Ghana Statistical Service, Accra

Gulacha MM, Mulungu DMM (2016) Generation of climate change scenarios for precipitation and temperature at local scales using SDSM in Wami-Ruvu River Basin Tanzania. Phys Chem Earth. https://doi.org/10.1016/j.pce.2016.10.003

Hashino T, Bradley AA, Schwartz SS (2007) Evaluation of bias-correction methods for ensemble streamflow volume forecasts. Hydrol

Earth Syst Sci 11: 939–950. http://www.hydrol-earth-syst-sci.net/11/939/2007/

Hatfield JL, Prueger JH (2015) Temperature extremes: effect on plant growth and development. Weather Clim Extremes 10:4–10

Heinzeller D, Olusegun C, Kunstmann H (2016a) High resolution (12 km) WRF-HADGEM2 daily outputs of simulated near-surface air temperature over West Africa, 1980–2009 (WASCAL Project). https://wascal-dataportal.org/geonetwork/?uuid=49499b53-a774-4679-be70-152a2401c02b. Accessed 25 June 2017

Heinzeller D, Olusegun C, Kunstmann H (2016b) High resolution (12 km) WRF-GFDL daily outputs of simulated near-surface air temperature over West Africa, 1980–2009 (WASCAL Project). https://wascal-dataportal.org/geonetwork/?uuid=cbcbda5f-7dda-4764-8783-e022a58e2885. Accessed 25 June 2017

Held IM, Soden BJ (2000) Water vapour feedback and global warming. Annu Rev Energy Environ 25(1):441–475. https://doi.org/10.1146/annurev.energy.25.1.441

Hoomehr S, Akinola AI, Wynn-Thompson T, Garnand W, Eick MJ (2018) Water temperature, pH, and road salt impacts on the fluvial erosion of cohesive streambanks. Water 10(302):1–16. https://doi.org/10.3390/w10030302

Hulme M, Barrow EM, Arnell NW, Harrison PA, Johns TC, Downing TE (1999) Relative impacts of human induced climate change and natural climate variability. Nature 397:688–691

Ibrahim B, Karambiri H, Polcher J, Yacouba H, Ribstein P (2014) Changes in rainfall regime over Burkina Faso under the climate change conditions simulated by 5 regional climate models. Clim Dyn 42(5–6):1363–1381

IPCC (1990) Climate change: the IPCC Scientific Assessment. Cambridge University Press, Cambridge, p 212

IPCC (2001) Climate change impacts adaptation and vulnerability. Intergovernmental Panel on Climate Change, (IPCC), Contribution of Working Group II to the third Assessment Report of IPCC. Cambridge University Press, Cambridge

IPCC (2007) Climate Change 2007: the physical science basis. Contribution of Working Group I to the Fourth Assessment Report of the Intergovernmental Panel on Climate Change. Cambridge University Press, Cambridge, p 996

IPCC (2014) Climate Change 2014: synthesis report. Contribution of Working Groups I, II and III to the Fifth Assessment Report of the Intergovernmental Panel on Climate Change (IPCC). IPCC, Geneva, p 151

Jeon S, Paciorek CJ, Wehner MF (2016) Quantile-based bias correction and uncertainty quantification of extreme event attribution statements. Weather Clim Extremes 12:24–32. https://doi.org/10.1016/j.wace.2016.02.001

Karl TR, Jones PD, Knight RW, Kukla G, Plummer N, Razuvayev V, Gallo K, Lindseay J, Charlson RJ, Peterson TC (1993) A new perspective on recent global warming: asymmetric trends of daily maximum and minimum temperature. Bull Am Meteorol Soc 74(6):1007–1023

Karl TR, Nicholls N, Ghazi A (1999) CLIVAR/GCOS/WMO workshop on indices and indicators for climate extremes: workshop summary. Clim Change 42:3–7

Kima SA, Okhimamhe AA, Kiema A, Zampaligre N, Sule I (2015) Adapting to the impacts of climate change in the sub-humid zone of Burkina Faso, West Africa: Perceptions of agro-pastoralists. Pastoralism Res Policy Pract 5(16):1–14. https://doi.org/10.1186/s13570-015-0034-9

Laprise R, Hernandez-Dıaz L, Tete K, Sushama L, Separovic´ L, Martynov A, Winger K, Valin M (2013) Climate projections over CORDEX Africa domain using the fifth-generation Canadian Regional Climate Model (CRCM5). Clim Dyn 41:3219–3246. https://doi.org/10.1007/s00382-012-1651-2

Leander R, Buishand AT, van den Hurk BJJM., de Wit MJM (2008) Estimated changes in flood quantiles of the river Meuse from resampling of regional climate model output. J Hydrol 351:331–343. https://doi.org/10.1016/j.jhydrol.2007.12.020

Ly M, Traore ST, Alhassane A, Sarr B (2013) Evolution of some observed climate extreme in the West African Sahel. Weather Clim Extremes 1:19–25

Machenhauer B, Windelband M, Botzet M, Jones RG, Déqué M (1996) Validation of present-day regional climate simulations over Europe: nested LAM and variable resolution global model simulations with observed or mixed layer ocean boundary conditions. Max Planck-Institut fur Meteorologie. Hamburg

Moriasi DN, Arnold JG, Van Liew MW, Bingner RL, Harmel RD, Veith TL (2007) Model evaluation guidelines for systematic quantification of accuracy in watershed simulations. Am Soc Agric Biol Eng 50(3):885 – 900

Muerth MJ, Gauvin St-Denis B, Ricard S, Velazquez JA, Schmid J, Minville M, Caya D, Chaumont D, Ludwig R, Turcotte R (2013) On the need for bias correction in regional climate scenarios to assess climate change impacts on river runoff. Hydrol Earth Syst Sci 17:1189–1204. https://doi.org/10.5194/hess-17-1189-2013

Murphy C, Charlton R (2006) Climate change impact on catchment hydrology and water resources for selected catchments in Ireland. In: National hydrology seminar, pp 38–49

Murphy A, Kapelle D (2014) Scaling up investment for ecosystem services to meet the global water crisis. Report presented to Nature Conservation Research Centre, Accra

New, M, Hewitson MB, Stephenson DB, Tsiga A, Kruger A, Manhique A, Gomez B, Coelho CAS, Masisi DN, Kululanga E, Mbambalala E, Adesina F, Saleh H, Kanyanga J, Adosi J, Bulane L, Fortunata L, Mdoka ML, Lajoie R (2006) Evidence of trends in daily climate extremes over Southern and West Africa. J Geophys Res 111:D14102. https://doi.org/10.1029/2005JD006289

Nikiema PM, Sylla MB, Ogunjobi K, Kebe I, Gibbaa P, Giorgid F (2016) Multi-model CMIP5 and CORDEX simulations of historical summer temperature and precipitation variabilities over West Africa. Int J Climatol. https://doi.org/10.1002/joc.4856

Nutsukpo DK, Jalloh A, Zougmoré R, Nelson GC, Thomas TS (2013) Ghana. In West African agriculture and climate change: a comprehensive analysis, chapter 6. International Food Policy Research Institute, Washington DC. http://ebrary.ifpri.org/cdm/ref/collection/p15738coll2/id/127450. Accessed 3 Jan 2018

Obuobie E, Kankam-Yeboah K, Amisigo B, Opoku-Ankomah Y, Ofori D (2012) Assessment of water stress in river basins in Ghana. J Water Clim Change 3(4):276–286. https://doi.org/10.2166/wcc.2012.030

Oktyabrskiy VP (2016) A new opinion of the greenhouse effect. St. Petersb Polytech Univ J Phys Math 2:124–126. https://doi.org/10.1016/j.spjpm.2016.05.008

Rasul G, Chaudhry QZ, Mahmood A, Hyder KW (2011) Effect of temperature rise on crop growth and productivity. Pak J Meteorol 8(15):53–62

Sakakibara Y, Owa K (2005) Urban–rural temperature differences in coastal cities: influence of rural sites. Int J Climatol 25:811–820

Smith JB, Pitts GJ (1997) Regional climate change scenarios for vulnerability and adaptation assessments. Clim Change 36:3–21

Teng J, Potter JN, Chiew FHS, Zhang L, Wang B, Vaze J, Evans JP (2015) How does bias correction of regional climate model precipitation affect modelled runoff? Hydrol Earth Syst Sci 19:711–728. https://doi.org/10.5194/hess-19-711-2015

Teutschbein C, Seibert J (2012) Bias correction of regional climate model simulations for hydrological climate-change impact studies: review and evaluation of different methods. J Hydrol 456–457:12–29

UICN/PACO (2010) Parks and reserves of Ghana: management effectiveness assessment of protected areas. UICN/PACO, Ouagadougou

UPEI (2017) Island database. Climate records for the day, and other database information. https://climate.upei.ca. Accessed 15 Feb 2017

Vanvyve E, Hall N, Messager C, Leroux S, Van Ypersele J (2008) Internal variability in a regional climate model over West Africa. Clim Dyn 30(2):191–202. https://doi.org/10.1007/s00382-007-0281-6

Vose RS, Easterling DR, Gleason B (2005) Maximum and minimum temperature trends for the globe: an update through 2004. Geophys Res Lett 32:L23822

Vuuren DP, Edmonds J, Kainuma M, Riahi K, Thomson A, Hibbard K, Hurtt GC, Kram T, Krey V, Lamarque JF, Masui T, Meinshausen M, Nakicenovic N, Smith SJ, Rose SK (2011) The representative concentration pathways: an overview. Clim Change 109(1–2):5–31. https://doi.org/10.1007/s10584-011-0148-z

Wigley TML, Jones PD, Briffa KR, Smith G (1990) Obtaining subgrid-scale information from course-resolution general circulation model output. J Geophys Res 95:1943–1953

Wilby RL, Dawson CW (2013) The Statistical DownScaling Model (SDSM): Insight from one decade of application. Int J Climatol 33:1707–1719

Wilby RL, Wigley TML (1997) Downscaling general circulation model output: a review of methods and limitations. Prog Phys Geogr 21(4):530–548

Wilby RL, Dawson CW, Murphy C, O'Conner P, Hawkins E (2014) The Statistical DownScaling Model-Decision Centric (SDSM-DC): conceptual basis and applications. Clim Res 61:251–268

WRC (2012) Pra River Basin—integrated water resources management plan. Water Resources Commission (WRC), Accra, p 53

Xu C-Y (1999) Climate change and hydrologic models: a review of existing gaps and recent research developments. Water Resour Manag 13(5):369–382

Zeleňákováa M, Purczb P, Hlavatác H, Blišťand P (2015) Climate change in urban versus rural areas. Procedia Eng 119:1171–1180

Zielinski S (2014) Why the city is (usually) hotter than the countryside. https://www.smithsonianmag.com/science-nature/city-hotter-countryside-urban-heat-island-science-180951985/#cdqCrUJx8UQkVMSt.99. Accessed 10 Jan 2018